

MOL #110650

**Long non-coding RNA LINC00657 acting as miR-590-3p
sponge to facilitate low concentration oxidized low-density
lipoprotein-induced angiogenesis**

Mei-hua Bao, Guang-yi Li, Xiao-shan Huang, Liang Tang, Li-ping Dong, Jian-ming Li

Department of Anatomy, Histology and Embryology; Science Research Center; Institute of
Neuroscience, Changsha Medical University, Changsha 410219, China; (M.-H. B., G.-Y.

L., L. T., L.-P. D., J.-M. L.)

Department of Pharmacology, Changsha Medical University, Changsha 410219,

China;(X.-S. H.)

MOL #110650

Running Title: LINC00657 promotes oxLDL-induced angiogenesis via miR590-3p

Correspondent Author:

Mei-hua Bao, Ph.D.

Department of Anatomy, Histology, and Embryology; Science Research Center;

Institute of Neuroscience; Changsha Medical University, Changsha, 410219, China;

Email: mhbao78@163.com; Tel:+86-731-8860-2602; Fax: 86-731-8860-2602

Number of text pages: 30

Number of tables: 0

Number of figures: 5

Number of references: 32

Number of words in the Abstract: 250

Number of words in the Introduction: 438

Number of words in the Discussion: 944

Abbreviations:

OxLDL: Oxidized low-density lipoprotein

HIF-1 α : Hypoxia-inducible factor (HIF)-1 α

VEGF: Vascular endothelial growth factor

MMP-2: Matrix Metalloproteinase-2

MMP-9: Matrix Metalloproteinase-9

lncRNA: Long non-coding RNA

HUVECs: Human umbilical vascular endothelial cells

DMEM: Dulbecco's modified Eagle's media

SDS-PAGE: Sodium dodecyl sulfate polyacrylamide gel electrophoresis

ELISA: Enzyme-Linked Immunosorbent Assay

MOL #110650

Abstract

Angiogenesis in atherosclerotic plaque promotes plaque growth, causes plaque hemorrhage and violates plaque stability. LINC00657 is a long noncoding RNA highly conserved and abundantly expressed in vascular endothelial cells. The present study was designed to investigate the effects and mechanisms of LINC00675 on low concentration of oxidized low-density lipoprotein (oxLDL) induced angiogenesis. Cell proliferation assay, transwell assay, wound healing assay, and tube formation assay were conducted to detect the effects of low concentration of oxLDL on angiogenesis; The results discovered that oxLDL promoted the cell proliferation, migration, and tube formation. OxLDL also up-regulated LINC00657 expression. Inhibition of LINC00657 by siRNA significantly suppressed the oxLDL-induced endothelial cell proliferation, migration, and tube formation. Bioinformatic assay indicated six binding sites in LINC00657 sequence to miR-590-3p. The up-regulation of LINC00657 was related to the down-regulation of miR-590-3p in oxLDL-treated endothelial cells; while down-regulation of LINC00657 resulted in up-regulation of miR-590-3p. The anti-angiogenesis effects of si-LINC00657 were partly abrogated by miR-590-3p inhibitor. Further dual-luciferase assay found miR-590-3p inhibited the expression of HIF-1 α by binding to the position of 689-696 in HIF-1 α 3'-UTR directly. MiR-590-3p also inhibited the oxLDL-induced up-regulation of HIF-1 α , VEGF, MMP-2, and MMP-9. These results suggested that in oxLDL treated endothelial cells, LINC00657 acted as a miR-590-3p sponge to attenuate the suppression of miR-590-3p on HIF-1 α , and to promote angiogenesis through VEGF,

MOL #110650

MMP-2, and MMP-9. The present study provided a new insight into the roles of LINC00657 and miR-590-3p on preventing oxLDL-induced angiogenesis and may provide a novel strategy for atherosclerosis treatment.

MOL #110650

1. Introduction

Atherosclerosis is a basis for many cardiovascular and cerebral vascular diseases, such as coronary artery disease, heart infarction and ischemic stroke (Hellings et al.,2010). The instability and rupture of atherosclerotic plaque are main reasons for many critical cardiovascular and cerebral vascular events. Recently, studies have demonstrated that the neovascularization in atherosclerotic plaque promoted plaque growth, leukocyte exchange, caused plaque hemorrhage and violated plaque stability (Camaré et al.,2017; Parma et al.,2017). However, methods to prevent the neovascularization process in atherosclerotic plaque are still limited.

In atherosclerotic lesions, local hypoxia happens commonly because of the thickening of the vessel wall, which blocked the oxygen exchange, and because of the increased oxygen consumption by high metabolic active cells such as macrophages (Bjornheden et al.,1999; Parathath et al.,2011). Hypoxia-inducible factor (HIF)-1 α is a transcriptional factor activated in the atherosclerotic plaque to adapt to the hypoxic environment. HIF-1 α activation subsequently promotes the production of vascular endothelial growth factor (VEGF), fibroblast growth factor, cytokines and angiopoietins (Hutter et al.,2013; Perrotta et al.,2015), which results in vascular inflammation and angiogenesis(Deng et al.,2016). Therefore, prevention of HIF-1 α might be an effective way to suppress neovascularization in atherosclerosis. Long non-coding RNAs (lncRNAs) are a group of non-coding RNAs with lengths >200nt, but without or with limited ability to encode proteins (International Human Genome Sequencing Consortium,2004). LINC00657 is a long intergenic non-coding RNA located in the chromosome 20q11.23, with the length of 5343bp (Liu et al.,2016). Studies

MOL #110650

have shown that LINC00657 is a highly conserved and abundantly expressed lncRNA in endothelial cells (Michalik et al.,2014). The expression of LINC00657 was up-regulated after hypoxia (Michalik et al.,2014), which inspires us to presume that LINC0657 might participate in the neovascularization in atherosclerosis.

MicroRNAs are another important group of non-coding RNAs with lengths of 18-24nt. Our previous studies have demonstrated the important roles of microRNAs in atherosclerosis (Bao et al.,2016, 2016). MiR-590-3p is a microRNA located on the chromosome 7 q11.23. MiR-590-3p was demonstrated to be involved in cancers, lipid metabolism, inflammation, and cardiac regeneration (Eulalio et al.,2012; Ge and Gong,2017). However, whether or not miR-590-3p participates in angiogenesis remains unclear. The previous study indicated that low concentration of oxLDL promoted angiogenesis (Yu et al.,2011). Our pilot experiments found oxidized low-density lipoprotein (oxLDL) treatment inhibited the expression of miR-590-3p and increased the expression of LINC00657. Bioinformatics has shown that LINC00657 contains six binding sites for miR-590-3p, which intrigues us to assume that LINC00657 might act as a miR-590-3p sponge. The present study was performed to investigate the effects and mechanisms of LINC00657 and miR-590-3p on the angiogenesis in human umbilical vascular endothelial cells (HUVECs) induced by low concentration ox-LDL.

2. Materials and Methods

2.1 Materials

HUVEC cell line was provided by the American Type Culture Collection

MOL #110650

(Manassas VA, USA); Dulbecco's modified Eagle's medium (DMEM) was obtained from Sigma (St. Louis, MO, USA); oxLDL was supplied by ThermoFisher Scientific (Grand Island, NY, USA); SYBR Green Premix DimerEraser kits, PrimeScript RT reagent Kit with gDNA Eraser (perfect real time) kits were purchased from Takara (Dalian, China); the primers were provided by Shanghai Sangon Biological Engineering Co. Ltd (Shanghai, China); mouse monoclonal antibody to HIF-1 α (ab113642) was purchased from Abcam (MA, USA); rabbit monoclonal antibody to VEGFR2 (#9698) and to β -actin (#8457) were purchased from Cell Signaling Technology (MA, USA); DAPI was obtained from Beyotime Institute of Biotechnology (Shanghai, China); Corning® Matrigel® Basement Membrane Matrix (catalog. 356234) was provided by Corning (NY, USA); si-LINC00657, si-NC, miR-590-3p mimics or inhibitor were obtained from RiboBio Co., Ltd (Guangzhou, China); Secrete-pair Dual Luminescence Assay Kit was provided by GeneCopoeia (Rockville, USA); pmir-REPORT luciferase vector (catalog. AM5795) was provided by ThermoFisher (MA, USA). The VEGF, MMP-2 and MMP-9 ELISA kit were purchased from Bosterbio Corp (Wuhan, China).

2.2 Cell culture and transfection

HUVECs were cultured in DMEM (low glucose) with 10% FBS; the cultivation environment was the humidified atmosphere with 5% CO₂ at 37 °C. The cells between passages 2 and 15 were used in this study.

For the transfection, lipofectamine 2000 was used to transfect miR-590-3p mimics, miR-590-3p inhibitor, si-LINC00657 and plasmids DNA. Briefly, the

MOL #110650

lipofectamine 2000, plasmids DNA, miR-590-3p mimics, and miR-590-3p inhibitor were diluted in Opti-MEM I Medium respectively and incubated for 5 min. After the incubation, the diluted lipofectamine 2000 was blended with diluted plasmids DNA, miR-590-3p mimics, and miR-590-3p inhibitor, respectively, and then was incubated for another 20 min at room temperature. The transfection mixtures were then added to cells and incubated for 6 hours. After that, the medium was replaced by fresh normal growth medium. The siRNAs in the present study are, si-LINC00657: 5'-TAG CCC TTC TAG ATG GAA A-3'; and si-NC: 5'-GCG CGA TAG CGC GAA TAT A-3', as reported previously(Lee et al.,2016).

2.3 Cell proliferation assay

For the cell proliferation assay, HUVECs were cultivated in a 96-well plate at a density of 5×10^3 cells per well. After treatment by different concentration of oxLDL (0, 5, 10, 50 $\mu\text{g}/\text{ml}$) for different time periods (0, 12, 24, 48h), the reagent MTS was added to each well according to the manufacturer's instructions. Cell proliferation was assessed by measuring the absorbance at 490nm using a plate reader.

2.4 Wound healing assay

The effects of LINC00657 on HUVECs migration were assessed by wound healing assays. The HUVECs were cultured in 12-well plate at a density of 5×10^5 cells/well. Cells were transfected with si-LINC00657 (1.2 μg) alone or with miR-590-3p inhibitor (100nM) for 24 hours, and then a yellow pipette tip was used to scrape a wound gap. The cells were carefully washed with PBS and treated with 10 $\mu\text{g}/\text{ml}$ oxLDL for another 48 hours. Three randomly selected regions were recorded

MOL #110650

using a microscope. The distance between cell boundaries was measured and the percentage of the wound gap that has been healed was calculated.

2.5 Transwell assay

To further assess the effects of LINC00657 on endothelial cell migration, transwell assay was performed. HUVECs were transfected firstly with si-LINC00657 (1.2 μ g) alone or with miR-590-3p inhibitor (100nM) for 24 hours as described in Section 2.2, and then were collected and added to the upper chamber of transwell in serum-free medium (4×10^4 endothelial cells per chamber). The lower chamber was filled with DMEM with 20% FBS. Then, oxLDL with the end concentration of 10 μ g/ml were added to the upper chamber, and the incubation of another 48 hours was performed. At the end of the incubation, cells were stained with DAPI and cells on the lower surface of the filter were photographed and counted under fluorescence microscope.

2.6 Tube formation assay

The capability of HUVECs to form capillary tube-like structures was assessed by the matrigel-based tube formation assay as previously described (Gonzalez-King et al., 2017). Firstly, HUVECs were transfected with si-LINC00657 and miR-590-3p inhibitor (100nM) for 24 hours as described in section 2.2. Then, 50 μ l of matrigel was added to a 96-well plate and solidified at 37 $^{\circ}$ C for 1 h. After that, the pre-transfected HUVECs were harvested and cultured on the matrigel-coated plate for another 24 hours, with or without oxLDL treatment. The tube formation effects were observed and photographed through the microscope. The tube-like structure length

MOL #110650

was calculated.

2.7 Real-time PCR for detection of LINC00657, miR-590-3p, *HIF1 α* , *VEGF*, *MMP-2* and *MMP-9*

As described previously (Bao et al.,2016), total RNA was extracted using TRIzol reagent (Invitrogen); then the total RNA was reversely transcribed to the complementary DNA using RT reagent Kit provided by Takara according to the manufacturer's instructions. Real-time PCR amplification reactions were conducted using the SYBR Premix DimerEraser™ (Perfect Real Time) assay kits, and the TL988-IV System (Tianlong, Xi'an, China). The real-time quantitative PCR program was an initial incubation at 95°C for 30 s, followed by 40 cycles of 95 °C 5 s, 60°C 30 s. The PCR primers are described as following: LINC00657: Forward: 5'- TGA TAG GAT ACA TCT TGG ACA TGG A -3', Reverse: 5'- AAC CTA ATG AAC AAG TCC TGA CAT ACA-3'; *HIF1 α* : Forward: 5'-CGT CGC TTC GGC CAG TGT GT -3', Reverse: 5'-TCC AGA GGT GGG GGT GCG AG-3'; *MMP-2*: Forward: 5'-GTT TCC ATT CCG CTT CCA GG-3', Reverse: 5'-TGC CCT TGA TGT CAT CCT GG-3'; *MMP-9*: Forward: 5'-GAC CTC AAG TGG CAC CAC CA-3', Reverse: 5'-GTG GTA CTG CAC CAG GGC AA-3'; *β -actin*: Forward: 5'-TGA CTG ACT ACC TCA TGA AGA T-3', Reverse: 5'-CAT GAT GGA GTT GAA GGT AGT T-3'. All samples were run in triplicate, and the results were analyzed using the $2^{(-\Delta\Delta C_t)}$ Method. For miR-590-3p, U6 was used as the internal reference, while for other genes, *β -actin* was used.

2.8 Western-blot assay for HIF-1 α

HUVECs were cultured and transfected as described in Section 2.2. After transfection, cells were treated with oxLDL (10 μ g/ml) for another 24 hours. After the treatment, the cells were collected and washed twice with PBS. The total proteins

MOL #110650

were extracted by adding 50 μ l RIPA lysis (with 1% PMSF and 10mM NaF) into the cells for 30min.

For the Western-blot assay, the total proteins were separated by the SDS-PAGE and transferred to PVDF membranes. After that, the membranes were blocked with 4% non-fat milk for 1 hour and then incubated with diluted HIF-1 α primary antibody for overnight at 4 °C. The membranes were afterward washed and incubated with 1:10000 dilution of the second antibody for 1 h and were detected with the enhanced chemiluminescence system. Relative intensities were analyzed by Quantity One^R software.

2.9 Enzyme-Linked Immunosorbent Assay (ELISA) detection of VEGF, MMP-2 and MMP-9 levels

HUVECs were cultured and transfected as described in Section 2.2. After transfection, cells were treated with oxLDL (10 μ g/ml) for another 24 hours. After treatment, the culture supernatants were collected and the level of VEGF, MMP-2, and MMP-9 were measured by the ELISA assay kits, following the instructions of the manufacturer.

2.10 HIF-1 α 3'-UTR (wild type and mutant) reporter plasmids construction, transfection and dual luciferase reporter analysis

The PCR was performed using primers specific for the HIF-1 α 3'-UTR (forward: 5'-GCCG CTC GAG GCT TTT TCT TAA TTT CAT TCC TTT TTTT GG-3'; reverse: 5'-GAA TGC GGC CGC GCC TGG TCC ACA GAA GAT GTT TAT TTG A-3'). The forward primers include a XhoI cutting site and the reverse primer contains a NotI cutting site. HUVEC cells genomic DNA was used as the template. The PCR products were digested with XhoI and NotI and cloned to pmir-REPORTTM luciferase vector

MOL #110650

(Ambion). The mutation at the potential binding site of miR-590-3p was performed using the QuikChange® Site-Directed Mutagenesis Kit (Stratagene, USA). The predicted miR-590-3p binding sites (underline) were changed as follows: wild type, 5'-UGGCAUUUAUUUGGAUAAAAUUC-3'; mutant type: 5'-UGGCAUUUAUUU GGAGACA CUCC-3'

For the transfection, HUVECs were cultured in a 24-well plate at the density of 5×10^4 cells/well for 24 hours. 400ng of wild type, mutant or blank plasmid DNA were co-transfected with 100 nM miR-590-3p or NC mimics. Dual luciferase reporter analysis was performed at 48 hours post-transfection using the Luciferase Assay kit according to the manufacturer's instructions (Promega).

2.11 Statistical analysis

All the statistics of three independent experiments were presented in the form of mean \pm S.D. The significance of the differences was analyzed by ANOVA followed by Newman-Student-Keuls test. A value of $P < 0.05$ is considered statistically significant.

3. Results

3.1 Effects of ox-LDL on cell viability and LINC00657 expression

LINC00657 was thought to be highly expressed in endothelial cells (Michalik et al., 2014). Our present study also found a high expression of LINC00657 in HUVECs (Figure 1A). After 24h treatment with different concentration of ox-LDL, the LINC00657 expression increased significantly ($P < 0.05$ vs. control). Relatively low concentration of ox-LDL (5, 10 $\mu\text{g/ml}$) treatment promoted the proliferation of HUVECs during the culture period, while high concentration of ox-LDL (50 $\mu\text{g/ml}$)

MOL #110650

inhibited the proliferation of HUVECs (Figure 1 B).

3.2 Effects of LINC00657 on ox-LDL-induced angiogenesis

In the present study, cell viability, wound healing, transwell, and tube formation assays were conducted to measure the function of LINC00657 on low concentration ox-LDL induced angiogenesis. As shown in Figure 1C, 24h and 48 h of ox-LDL (10 μ g/ml) treatment stimulated the growth of HUVECs significantly, and LINC00657 inhibition by siRNA suppressed the cell growth induced by ox-LDL. Transwell assay found 48 h of ox-LDL treatment promoted the migration of HUVECs from the upper chamber to the lower chamber (about 2.5 folds of control), and si-LINC00657 inhibited ox-LDL-induced cell migration (Figure 1 D, E). We also found ox-LDL facilitated the tube formation and wound healing of HUVECs, and si-LINC00657 suppressed the alteration (Figure 1 F-I).

3.3 Si-LINC00657 promoted the expression of miR-590-3p

To explore the mechanisms of LINC00657, we analyzed its sequence and found it contained six binding sites with miR-590-3p (Figure 2 A). Therefore, we have assessed whether LINC00657 acts as competitive endogenous RNA to miR-590-3p, and inhibits the expression of miR-590-3p. As shown in Figure 2 B, si-LINC00657 significantly down-regulated the level of LINC00657 (32.9% of control group). The inhibition of LINC00657 resulted in a dramatical induction of miR-590-3p (4.5 folds of control, Figure 2 C). OxLDL (10 μ g/ml) treatment for 24 hours promoted the expression of LINC00657, while down-regulated the expression of miR-590-3p (Figure 2 D).

MOL #110650

3.4 Inhibition of miR-590-3p partly abrogated the effects of LINC00657 on ox-LDL induced angiogenesis

To verify whether the anti-angiogenesis effects of LINC00657 are mediated by miR-590-3p, we have detected the effects of miR-590-3p inhibitor on anti-angiogenesis of si-LINC00657. The inhibition of miR-590-3p by inhibitor abrogated the suppression of angiogenesis by si-LINC00657 in oxLDL treated HUVECs (Figure 3A). We also found si-LINC0657 suppressed the endothelial cells transwell migration, the tube formation, and wound healing. And all these effects were suppressed by a certain degree by miR-590-3p inhibition (Figure 3 B-G). These results indicate that the si-LINC00675 might play its role in angiogenesis through miR-590-3p.

3.5 Target identification for miR-590-3p

In order to figure out the mechanism for the effects of miR-590-3p, we predicted the targets for miR-590-3p by bioinformatics. As shown in Figure 4 B, miR-590-3p is predicted to bind to the position 689 to 696 of HIF-1 α 3'-UTR. To verify this prediction, a dual luciferase reporter assay was performed. The results showed that in HUVECs, miR-590-3p mimics significantly inhibited the luciferase activity, while miR-590-3p inhibitor promoted it (Figure 4A). The mutation of the binding position of HIF-1 α eliminated the effects of miR-590-3p. In order to further verify the regulation of miR-590-3p to HIF-1 α , we tested the HIF-1 α levels after miR-590-3p over-expression and inhibition. As shown in Figure 4 C-E, the over-expression of miR-590-3p in HUVECs inhibited the expression of HIF-1 α both in mRNA and

MOL #110650

protein level.

3.6 Effects of miR-590-3p on HIF1 α , VEGF, MMP-2, MMP-9 expression

HIF-1 α is widely considered to be a transcriptional factor which regulates many angiogenesis-related genes, such as VEGF and MMPs. In the present study, qPCR, WB and ELISA were used to investigate the effects of miR-590-3p on *HIF-1 α* , *VEGF*, *MMP-2* and *MMP-9* mRNA and protein expression with and without oxLDL. As shown in Figure 4 F-I, miR-590-3p significantly suppressed both the mRNA and protein levels of HIF-1 α , VEGF, MMP-2 and MMP-9 in HUVECs. When the endothelial cells were treated with low concentration of oxLDL, the expression of HIF-1 α , VEGF, MMP-2, and MMP-9 increased. MiR-590-3p over-expression suppressed the oxLDL-induced increase of these factors.

Discussion

Our present study found that low concentration of oxLDL promoted the proliferation, migration, and tube formation of HUVECs, as well as the expression of LINC00657. Inhibition of LINC00675 by siRNA suppressed the oxLDL induced angiogenesis and expression of miR-590-3p. Moreover, the effects of si-LINC00657 were partly abrogated by the miR-590-3p inhibitor. Further studies found miR-590-3p inhibited the expression of HIF-1 α by directly targeting the position of 689-696 in HIF-1 α 3'-UTR. The inhibition of HIF-1 α subsequently decreased the production of VEGF, MMP-2, MMP-9, which may contribute to the angiogenesis caused by low concentration of oxLDL during atherosclerosis.

OxLDL has long been considered as a major risk factor for endothelial cell

MOL #110650

dysfunction and death in atherosclerosis. However, studies also found low concentration of oxLDL promoted angiogenesis (Dandapat et al., 2007; Yu et al., 2011; Khaidakov et al., 2012). VEGF expression, redox-sensitive pathways, and nitric oxide synthesis were thought to be involved in the pro-angiogenesis effects of oxLDL (Dandapat et al., 2007; Yu et al., 2011; Khaidakov et al., 2012). Our present study verified that low concentration of oxLDL (5, 10 µg/ml) promoted the growth of HUVECs. 10 µg/ml oxLDL induced the transwell migration, tube formation and wound healing characteristics of endothelial cells. Besides, we furthermore found the low concentration of oxLDL (10 µg/ml) treatment increased the production of pro-angiogenesis factors, such as VEGF, MMP-2, and MMP-9. VEGF is a strong stimulator for both physiological and pathological angiogenesis (Ribatti et al., 2001). MMP-2 and MMP-9 are two most important members of MMPs family for extracellular matrix degradation, which facilitate the endothelial cell migration and angiogenesis (Liu et al., 2014) [25, 26]. We found in our study that low concentration of oxLDL increased the expression of VEGF, MMP-2, and MMP-9, consistent with previous reports (Dandapat et al., 2007; Tsai et al., 2016). These might partly explain the pro-angiogenesis effects of low concentration oxLDL on ECs.

To explore the mechanisms of oxLDL-induced angiogenesis, we focused on one lncRNA, LINC00657. LINC00657, also called noncoding RNA activated by DNA damage (NORD), is a 5.3 kb intergenic long noncoding RNA broadly and abundantly expressed in human tissues, including endothelial cells (Michalik et al., 2014; Lee et al., 2016; Liu et al., 2016). The high expression of LINC00657 is related to the breast

MOL #110650

cancer cell growth and proliferation(Liu et al.,2016). In endothelial cells, LINC00657 is highly expressed in the cytoplasm (Michalik et al.,2014). Hypoxia (0.2% O₂) induced the expression of LINC00657 to 2.5 folds compared with normoxia(Michalik et al.,2014). OxLDL is an oxidatively modified product of low-density lipoprotein. OxLDL results from oxidative burst during infection or other oxidative pathological processes. On the other hand, oxLDL also promotes oxidative stress, which is involved in the pathogenesis of atherosclerosis (Ishigaki et al.,2009; Peluso et al.,2012). Since hypoxia and high level of oxLDL exist in the atherosclerotic lesion, we, therefore, presume that LINC00657 might participate in the pathogenesis of atherosclerosis. And oxLDL-induced oxidative stress may cause an altered expression of LINC00657. Our present study found a significant increase in LINC00657 expression after oxLDL treatment. The inhibition of LINC00657 by siRNA suppressed oxLDL induced cell proliferation, migration, tube formation and wound healing ability. These results demonstrated that LINC00657 is involved in the pro-angiogenesis effects of oxLDL. But the details of the mechanism of how hypoxia or oxLDL promote the LINC00657 expression are still unclear.

LncRNAs play their roles through many mechanisms including transcriptional and post-transcriptional regulation, sources of small RNAs, miRNA sponges, mRNA binders, and protein binders, *etc.*(Kornienko et al.,2013) The bioinformatic analysis found six binding sites on LINC00657 with miR-590-3p. LINC00657 is reported to exist in the cytoplasm (Michalik et al.,2014). We found that inhibition of LINC00657 by siRNA promoted the expression of miR-590-3p, while the increase of LINC00657

MOL #110650

in oxLDL treated endothelial cells was related to the decrease of miR-590-3p. Further research found miR-590-3p inhibitor abrogated the effects of si-LINC00657 on oxLDL induced angiogenesis. These results demonstrated that the LINC00657 might interact with miR-590-3p and interfere with the process of angiogenesis.

MiR-590-3p is a microRNA located at the position of chromosome 7 q11.23. The functions of miR590 have been discovered in recent years. Both miR590-5p and miR-590-3p were found to participate in the carcinogenesis of different cancers, such as prostate cancer, liver cancer, lung cancer, *etc.*(Wang et al.,2016; Chen et al.,2017; Ge and Gong,2017). A most recent study found miR590-5p inhibited colorectal cancer angiogenesis through NF90/VEGFA signal(Zhou et al.,2016). However, the effects of miR-590-3p on angiogenesis are still unclear. Our study found a significant decrease of miR-590-3p in HUVECs after oxLDL treatment. Bioinformatics predicts miR-590-3p may bind to the position of 689-696 in HIF-1 α 3'-UTR. Further dual luciferase reporter analysis and western-blot analysis verified the interaction between miR-590-3p and HIF-1 α .

HIF-1 α is a transcriptional factor reported to be activated by oxLDL[27]. The activation of HIF-1 α promotes the expression of many growth factors and cytokines, regulates cell proliferation and survival, and is involved in biological processes such as angiogenesis(Lee et al.,2004; Sun et al.,2010). Therefore, the regulation of miR-590-3p on HIF-1 α might responsible for the effects of miR-590-3p on angiogenesis. Our present results demonstrated an increase in HIF-1 α expression after oxLDL treatment, which subsequently increased the production of VEGF, MMP-2,

MOL #110650

and MMP-9. Mir-590-3p up-regulation inhibited the oxLDL-induced HIF-1 α , VEGF, MMP-2 and MMP-9 expression, indicating the functionalities of miR-590-3p might be partly obtained through the HIF-1 α signal.

In conclusion, our results suggest that in ECs, low concentration of oxLDL promote the expression of LINC00657; the LINC00657 act as ceRNA and inhibit the expression of miR-590-3p, which then loses its suppression on HIF-1 α . The up-regulation of HIF-1 α promotes the expression of VEGF, MMP-2, MMP-9 and eventually induces the angiogenesis (Figure 5). Our present study provides a new insight into the roles of LINC00657 and miR-590-3p on oxLDL-induced angiogenesis and may provide a novel strategy for atherosclerosis treatment.

Authorship Contributions:

Participated in research design: Bao M.H., and Li J.M.

Conducted experiments: Bao M.H., Li G.Y., and Huang X.S.

Performed data analysis: Tang L., and Dong L.P.

Wrote or contributed to the writing of the manuscript: Li J.M., and Bao M.H.

All authors reviewed the manuscript.

MOL #110650

References

- Bao, M.H.; Li, J.M.; Luo, H.Q.; Tang, L.; Lv, Q.L.; Li, G.Y.; Zhou, H.H. NF- κ B-Regulated miR-99a Modulates Endothelial Cell Inflammation. *Mediators Inflamm.* **2016**, 2016, 5308170.
- Bao, M.H.; Li, J.M.; Zhou, Q.L.; Li, G.Y.; Zeng, J.; Zhao, J.; Zhang, Y.W. Effects of miR-590 on oxLDL-induced endothelial cell apoptosis: Roles of p53 and NF- κ B. *Mol Med Rep* **2016**, 13, 867-873.
- Bao MH, Li JM, Luo HQ, et al. NF-kappaB-Regulated miR-99a Modulates Endothelial Cell Inflammation. *Mediators Inflamm.* 2016. 2016: 5308170.
- Bjornheden T, Levin M, Evaldsson M, Wiklund O. Evidence of hypoxic areas within the arterial wall in vivo. *Arterioscler Thromb Vasc Biol.* 1999. 19(4): 870-6.
- Camaré C, Pucelle M, Nègre-Salvayre A, Salvayre R. Angiogenesis in the atherosclerotic plaque. *Redox Biol.* 2017. 12: 18-34.
- Chen H, Luo Q, Li H. MicroRNA-590-3p promotes cell proliferation and invasion by targeting inositol polyphosphate 4-phosphatase type II in human prostate cancer cells. *Tumour Biol.* 2017. 39(3): 1010428317695941.
- Dandapat A, Hu C, Sun L, Mehta JL. Small concentrations of oxLDL induce capillary tube formation from endothelial cells via LOX-1-dependent redox-sensitive pathway. *Arterioscler Thromb Vasc Biol.* 2007. 27(11): 2435-42.
- Deng W, Feng X, Li X, Wang D, Sun L. Hypoxia-inducible factor 1 in autoimmune diseases. *Cell Immunol.* 2016. 303: 7-15.
- Eulalio A, Mano M, Dal Ferro M, et al. Functional screening identifies miRNAs inducing cardiac regeneration. *Nature.* 2012. 492(7429): 376-81.
- Ge X, Gong L. MiR-590-3p suppresses hepatocellular carcinoma growth by targeting TEAD1. *Tumour Biol.* 2017. 39(3): 1010428317695947.
- Gonzalez-King H, Garcia NA, Ontoria-Oviedo I, Ciria M, Montero JA, Sepulveda P. Hypoxia inducible factor-1 alpha potentiates Jagged 1-mediated angiogenesis by mesenchymal stem cell-derived exosomes. *Stem Cells.* 2017 .
- Hellings WE, Peeters W, Moll FL, et al. Composition of carotid atherosclerotic plaque is associated with cardiovascular outcome: a prognostic study. *Circulation.* 2010. 121(17): 1941-50.
- Hutter R, Speidl WS, Valdiviezo C, et al. Macrophages transmit potent proangiogenic effects of oxLDL in vitro and in vivo involving HIF-1 α activation: a novel aspect of angiogenesis in atherosclerosis. *J Cardiovasc Transl Res.* 2013. 6(4): 558-69.
- International Human Genome Sequencing Consortium. Finishing the euchromatic sequence of the human genome. *Nature* **2004**, 431, 931-945.
- Ishigaki Y, Oka Y, and Katagiri H (2009) Circulating oxidized LDL: a biomarker and a pathogenic factor. *Curr Opin Lipidol* **20**: 363-369.
- Khaidakov M, Mitra S, Wang X, et al. Large impact of low concentration oxidized LDL on angiogenic potential of human endothelial cells: a microarray study. *PLoS One.* 2012. 7(10): e47421.
- Kornienko AE, Guenzl PM, Barlow DP, Pauler FM. Gene regulation by the act of long non-coding RNA transcription. *BMC Biol.* 2013;11:59.
- Lee JW, Bae SH, Jeong JW, Kim SH, Kim KW. Hypoxia-inducible factor (HIF-1)alpha: its protein stability and biological functions. *Exp. Mol. Med.* 2004;36:1-12.
- Lee, S.; Kopp, F.; Chang, T.C.; Sataluri, A.; Chen, B.; Sivakumar, S.; Yu, H.; Xie, Y.; Mendell, J.T. Noncoding

MOL #110650

- RNA NORAD Regulates Genomic Stability by Sequestering PUMILIO Proteins. *Cell* **2016**, 164, 69-80.
- Liu G, Liu M, Wei J, et al. CS5931, a novel polypeptide in *Ciona savignyi*, represses angiogenesis via inhibiting vascular endothelial growth factor (VEGF) and matrix metalloproteinases (MMPs). *Mar Drugs*. 2014. 12(3): 1530-44.
- Liu, H.; Li, J.; Koirala, P.; Ding, X.; Chen, B.; Wang, Y.; Wang, Z.; Wang, C.; Zhang, X.; Mo, Y.Y. Long non-coding RNAs as prognostic markers in human breast cancer. *Oncotarget* **2016**, 7, 20584-20596.
- Michalik, K.M.; You, X.; Manavski, Y.; Doddaballapur, A.; Zörnig, M.; Braun, T.; John, D.; Ponomareva, Y.; Chen, W.; Uchida, S.; Boon, R.A.; Dimmeler, S. Long noncoding RNA MALAT1 regulates endothelial cell function and vessel growth. *Circ. Res.* **2014**, 114, 1389-1397.
- Parathath S, Mick SL, Feig JE, et al. Hypoxia is present in murine atherosclerotic plaques and has multiple adverse effects on macrophage lipid metabolism. *Circ Res*. 2011. 109(10): 1141-52.
- Parma L, Baganha F, PHA Q, de Vries MR. Plaque angiogenesis and intraplaque hemorrhage in atherosclerosis. *Eur J Pharmacol*. 2017 .
- Peluso I, Morabito G, Urban L, Ioannone F, and Serafini M (2012) Oxidative stress in atherosclerosis development: the central role of LDL and oxidative burst. *Endocr Metab Immune Disord Drug Targets* **12**: 351-360.
- Perrotta I, Moraca FM, Sciangula A, Aquila S, Mazzulla S. HIF-1 α and VEGF: Immunohistochemical Profile and Possible Function in Human Aortic Valve Stenosis. *Ultrastruct Pathol*. 2015. 39(3): 198-206.
- Ribatti D, Nico B, Morbidelli L, et al. Cell-mediated delivery of fibroblast growth factor-2 and vascular endothelial growth factor onto the chick chorioallantoic membrane: endothelial fenestration and angiogenesis. *J Vasc Res*. 2001. 38(4): 389-97.
- Sun X, Wei L, Chen Q, Terek RM. CXCR4/SDF1 mediate hypoxia induced chondrosarcoma cell invasion through ERK signaling and increased MMP1 expression. *Mol. Cancer* 2010;9:17.
- Tsai KL, Chang YL, Huang PH, Cheng YH, Liu DH, Chen HY, Kao CL. Ginkgo biloba extract inhibits oxidized low-density lipoprotein (oxLDL)-induced matrix metalloproteinase activation by the modulation of the lectin-like oxLDL receptor 1-regulated signaling pathway in human umbilical vein endothelial cells. *J. Vasc. Surg.* 2016;63:204-15.e1.
- Wang FF, Wang S, Xue WH, Cheng JL. microRNA-590 suppresses the tumorigenesis and invasiveness of non-small cell lung cancer cells by targeting ADAM9. *Mol Cell Biochem*. 2016. 423(1-2): 29-37.
- Yu S, Wong SL, Lau CW, Huang Y, Yu CM. Oxidized LDL at low concentration promotes in-vitro angiogenesis and activates nitric oxide synthase through PI3K/Akt/eNOS pathway in human coronary artery endothelial cells. *Biochem Biophys Res Commun*. 2011. 407(1): 44-8.
- Zhou Q, Zhu Y, Wei X, et al. MiR-590-5p inhibits colorectal cancer angiogenesis and metastasis by regulating nuclear factor 90/vascular endothelial growth factor A axis. *Cell Death Dis*. 2016. 7(10): e2413.

MOL #110650

Footnotes:

E-Mails:

mhbao78@163.com (M.-H. B.); liguangyi1977@163.com (G.-Y.L.); tlcool318@163.com (L.T.);
huangxiaoshan0123@yeah.net (X.-S. H); ddongliping@163.com (L.-P.D.);
ljming0901@sina.com (J.-M.L.)

The present study was supported by the Construct Program of the Key Discipline in Hunan Province, National Sciences Foundation of China [Grant No. 81670427], the Foundation of Hunan Educational Committee [Grant No. 15C0146, 5B031 and 15A023], Hunan Provincial Natural Science Foundation[Grant No. 2015JJ6010], Basic Research Program of Science and Technology Commission Foundation of Hunan province [Grant No. 2015JC3059].

MOL #110650

Figure legends:

Figure 1 Effects of ox-LDL and LINC00657 on endothelial cell angiogenesis. A, the effects of different concentration of oxLDL on LINC00657 expression in HUVEC. B, the influence of different concentrations of ox-LDL on cell viability in different time. C, the effects of si-LINC00657 on oxLDL-induced cell viability change; cell viability in different time. HUVECs were transfected with si-LINC00657 or siNC respectively for 24 h and then treated with ox-LDL (10 μ g/ml) for the indicated time. Cell viability was assessed by MTS method. D, E, Transwell assay for cell migration. HUVECs were transfected with si-LINC00657 (100 nM) or siNC respectively for 24 h and then treated with ox-LDL (10 μ g/ml) for another 48 h. The cells in the lower chamber were stained with DAPI and calculated. F, Tube formation assay. G, Wound healing assay. A linear wound was made, and ox-LDL and/or si-LINC00657 were added, and the distance between the cell boundaries was measured. H, Relative length of endothelial cell tube formation. Tube length was quantified in three random microscope fields, and normalized relative to the NC group; I, Percentage of the healed wound. Data are Mean \pm SD from 3 independent experiments, * P <0.05, ** P <0.01, compared with NC; # P <0.05 compared with the ox-LDL group.

Figure 2 Regulation of LINC00657 on miR-590-3p expression. A, the alignment of LINC00657 and miR-590-3p; B, effects of si-LINC00657 on LINC00657 expression. HUVECs were cultured in 24-well plates, and transfected with 500ng of

MOL #110650

si-LINC00657. The expression of LINC00657 was measured by qPCR. C, effects of si-LINC00657 on miR-590-3p expression. D, the expression of LINC00657 and miR-590-3p after oxLDL treatment for 24 hours. Data are Mean \pm SD from 3 independent experiments, $**P<0.01$, compared with control.

Figure 3 Inhibition of miR-590-3p partly abrogated the effects of LINC00657 on ox-LDL induced angiogenesis. A, Cell viability measured by MTS method. B, C, Transwell assay for cell migration. D, Tube formation assay. E, Wound healing assay. F, Relative length of endothelial cell tube formation. Tube length were quantified in three random microscope fields, and normalized relative to the NC group; G, Percentage of the healed wound. Data are Mean \pm SD from 3 independent experiments, $**P<0.01$, compared with the oxLDL+si-NC group; $^{\#}P<0.05$ compared with the ox-LDL+si-LINC00657 group.

Figure 4 The regulation of miR-590-3p on HIF-1 α , VEGF, MMP-2, MMP-9 expression. A, The relative luciferase activities measured by dual luciferase reporter analysis. B, The predicted miR-590-3p binding site in HIF-1 α . C, the effects of miR-590-3p on HIF-1 α protein expression. D, The mRNA expression of HIF-1 α . E, the normalized level of HIF-1 α protein. F, the effects of miR-590-3p on oxLDL-induced *HIF-1 α* , *VEGF*, *MMP-2* and *MMP-9* mRNA expression; G, the effects of miR-590-3p on oxLDL-induced HIF-1 α protein expression; H, the normalized level of HIF-1 α and VEGFR2 protein; I, ELISA analysis of VEGF,

MOL #110650

MMP-2 and MMP-9 levels in HUVECs culture supernatant. Data are Mean \pm SD from 3 independent experiments, * P <0.05, ** P <0.01 vs NC; # P <0.05 vs oxLDL.

Figure 5 Function of LINC00657 in oxLDL-induced angiogenesis. In endothelial cells, low concentration of oxLDL promotes the expression of LINC00657; the LINC00657 acts as miRNA sponge and inhibited the level of miR-590-3p; miR-590-3p losses its suppression on HIF-1 α , and leads to the up-regulation of HIF-1 α ; HIF-1 α then promotes the expression of VEGF, MMP-2, MMP-9 and eventually induced the angiogenesis.

Figure 1

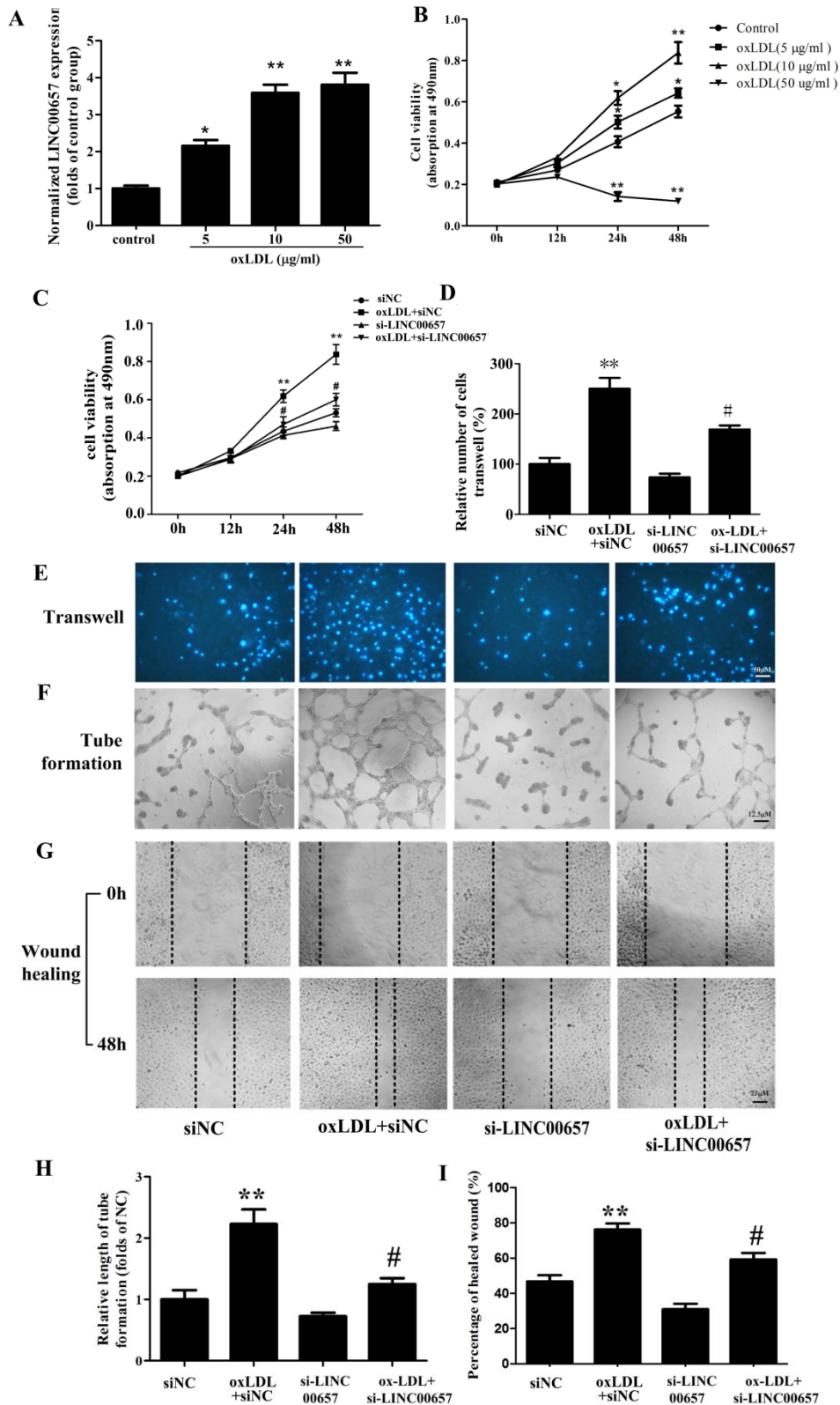


Figure 2

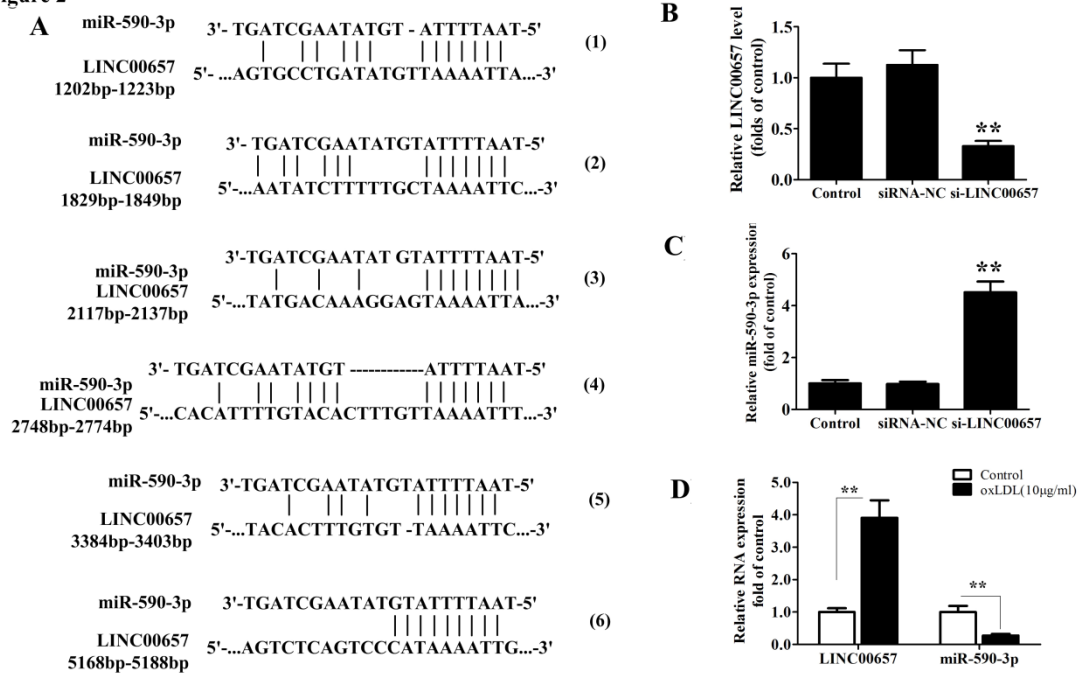


Figure 3

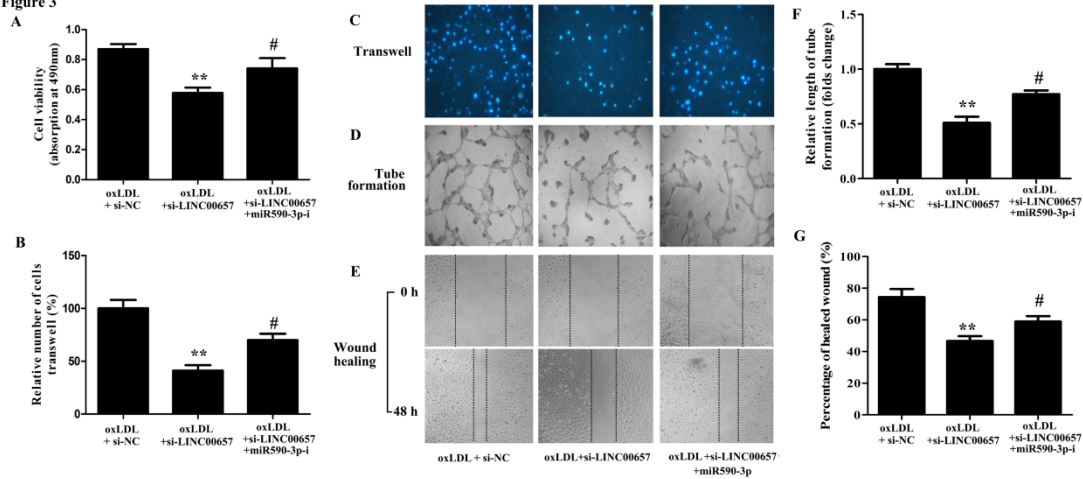


Figure 4

